Springer

KSME

Journal of Mechanical Science and Technology 28 (9) (2014) 3537~3544
www.springerlink.com/content/1738-494x
DOI 10.1007/s12206-014-0814-y

A novel method for identifying rotor-stator rubbing positions using the cepstrum analysis technique †

Guo Chen[1,*], Yong-Quan Liu[2], Guang-Yi Jiang[2], Cheng-Gang Li[2], Guo-Quan Feng[2] and De-You Wang[2]

[1]*College of Civil Aviation, Nanjing University of Aeronautics and Astronautics, Nanjing, 210016, China*
[2]*Shenyang Aero-engine Design Institute, Aviation Industry Corporation of China, Shenyang, 110015, China*

(Manuscript Received August 14, 2013; Revised February 23, 2014; Accepted June 3, 2014)

Abstract

A novel method of aero-engine rubbing positions identification based on cepstrum analysis is proposed, and the transfer path characteristics which reflect the transfer characteristics information from rubbing points to casing measuring points are separated from the vibration acceleration signals of casing by means of cepstrum analysis. Therefore, there is different transfer characteristics information at different rubbing positions, and in view of this, twenty rubbing positions identification features from the cepstrum are extracted. A large number of rubbing experiments of different positions are simulated with the rotor experiment rig of aero-engine, and the characteristic analysis of experimental samples at different rubbing positions is carried out, and the results indicate the consistency of features to the same rubbing position and the difference of the features to the different rubbing positions. Finally, the aero-engine rubbing positions identification is carried out using the nearest neighbor classification method, the recognition rate reaches 100%, and the effectiveness of the method is full verified.

Keywords: Aero-engine; Rotor-stator rubbing; Rubbing position identification; Cepstrum analysis; Transfer path

1. Introduction

Rotor-stator rubbing fault is a common strongly nonlinear fault in high speed rotating machinery including aero-engine [1]. At present, researches mostly focus on how to judge whether the rubbing fault appears or not, while, few researches pay attention to the recognition of the rubbing positions.

Ref. [2] recognized the location of rubbing positions, by using the stator vibration signals as the diagnosis source, which are combined with the angle location signals, extracting the enveloping signals of stators from the natural high frequency vibration by means of the methods such as the resonance demodulation, the Fourier transform and the Hilbert transform. Ref. [3] combined the acoustic emission technique with the wavelet packet and the cross-correlation, and determined the rubbing positions by comparing the correlation coefficients. Ref. [4] proposed a energy attenuation model using the characteristics of acoustic emission signals, transformed the location problem to estimation problem, approximated the source positions by means of adaptive subgradient projection system estimation algorithm, and finally recognized the rubbing location. Ref. [5] studied rubbing positions recognition of rotor system according to the difference of dynamic stiffness between rubbing points and non rubbing points. Ref. [6] transformed the parameter identification problems of rubbing positions to multi-parameter optimization problem, identified the rubbing positions by using the genetic algorithm to optimize solution according to the established rotor system finite element model with rubbing fault. Ref. [7] studied the propagation characteristics of acoustic emission signals using the lamb wave theory, established the near-field acoustic emission beam-forming method, and recognized the rotor-stator rubbing location using this method. Ref. [8] used the wavelet transform method to decompose the acoustic emission signals into different frequency ranges in order to eliminate the effect of the acoustic emission noises, and realized the rubbing fault location by combining with the autocorrelation function method. Ref. [9] improved the sphere support vector machines and used them to carry out the shaft rubbing positions identification. Ref. [10] realized the rubbing positions location according to the nonlinear frequency response function and the rotor system finite element model.

However, these methods are very difficult to be applied to engineering practice because their testing means are uncommon, too complex, and they do not consider the practical structures and rubbing characteristics of aero-engine.

*Corresponding author. Tel.: +86 25 84891850, Fax.: +86 25 84891850
E-mail address: cgzyx@263.net
† Recommended by Associate Editor Kyung-Soo Kim

For the modern large-scale aero-engines, the main causes of rubbing are the unbalance of rotors, deformation of casings, and misalignment of supports and so on. Because of the rotor's high-weight, and the casing's light-weight due to its thin-walled structure, the rubbing force can hardly make the rotors rebound. Therefore, the rubbing positions are basically at the fixed positions of the casings. However, the rubbing positions will change with the casing deformation and the directions of support misalignment varying. Therefore, effective diagnosis and identification to rubbing positions have great significance for revealing the rubbing causes and improving the design of aero-engine.

In view of this, in this paper, a novel method for identifying rotor-stator rubbing positions using the cepstrum analysis technique is proposed. The information which reflects the transfer characteristics of rubbing positions is separated from the vibration acceleration signals of casing measuring points by means of cepstrum analysis, and the features for rubbing positions identification are extracted. A large number of rubbing experiments of different positions are simulated with the rotor experiment rig of aero-engine, and the correctness and effectiveness of the new method are full verified by the experimental data.

2. Features extraction of rotor-stator rubbing positions identification based on the cepstrum analysis

Suppose that the continuous signal $x(t)$ is sampled, and the sampling period is T_s, and the time series $x(n)$ with N points is obtained, n = 1,2,…N. Then, according to the fast Fourier transform (FFT), $X(k)$ = DFT[$x(n)$], in which DFT[.] is the discrete Fourier transform and the frequency spectrum intervals is $\Delta f = 1/(N \cdot T_s)$. Using the $X(k)$, k = 1,2,…N, then the power spectral density function can be calculated, namely:

$$\begin{aligned} S_{xx}(k) &= \frac{1}{N} \cdot T_s \cdot X^*(k) X(k) \\ &= \frac{1}{N} \cdot T_s \cdot \left\| X(k) \right\|^2 . \end{aligned} \tag{1}$$

The power cepstrum is generally used in the engineering practice, and it is defined as the inverse Fourier transform after taking logarithm of power spectral density function, in which, IDFT[.] denotes the inverse discrete Fourier transform, namely:

$$C_x(k) = \mathrm{IDFT}[\lg(S_{xx}(k))] . \tag{2}$$

Suppose $x(n)$ is the collected response signal, and its frequency spectrum is $X(k)$; rubbing force at rubbing points is $f(n)$ and its frequency spectrum is $F(k)$; frequency response function from the rubbing points to the measuring points is $h(n)$, and its frequency spectrum is $H(k)$; in which, n, k = 1, 2,…N, then, according to the response characteristics of linear system,

$$X(k) = F(k)H(k), k = 1,2,\cdots,N . \tag{3}$$

From Eqs. (1)~(3), the power cepstrum can be obtained as shown in Eq. (4),

$$\begin{aligned} C_x(k) &= \mathrm{IDFT}[\lg(S_{xx}(k))] \\ &= \mathrm{IDFT}\left[\lg(\frac{1}{N} \cdot T_s \cdot \left\| X(k) \right\|^2) \right] \\ &= \mathrm{IDFT}\left[\lg\left(\frac{1}{N} \cdot T_s \cdot \left\| H(k)F(k) \right\|^2 \right) \right] \\ &= \mathrm{IDFT}\left[\lg\left(\frac{1}{N} \cdot T_s \cdot \left\| H(k) \right\|^2 \cdot \left\| F(k) \right\|^2 \right) \right] \\ &= \mathrm{IDFT}\left[\log\left(T_s / N \right) \right] + 2\mathrm{IDFT}\left[\log\left(\left\| F(k) \right\| \right) \right] \\ &\quad + 2\mathrm{IDFT}\left[\log\left(\left\| H(k) \right\| \right) \right] . \end{aligned} \tag{4}$$

From the Eq. (4), it can be seen that, the rubbing exciting force source are separated from the transfer path from the rubbing point to the measuring point in the power cepstrum $C_x(k)$. In Eq. (4), the first term is the zero quefrency components, the second term is the quefrency component of the rubbing exciting force, and the third term is the quefrency component of the transfer path from the rubbing point to the measuring point.

The quefrency is time dimension. In cepstrum, the transfer characteristics are mainly reflected in the low quefrency sections and the excitation characteristics are mainly reflected in the high quefrency sections. Therefore, in order to extract the information reflecting the transfer characteristics from the rubbing point to the measuring point, the several cepstrum points in the low quefrency sections should be used as the characteristics which reflect the transfer path. In this paper, the real part of the following 20 cepstrum points after the zero quefrency point are extracted as the features, accordingly, the feature vector for rubbing positions identification is formed.

3. Rubbing experiments

Traditional rubbing experiments do not consider the thin-walled structure of aero-engine and the rotor disc-blade structure, therefore the rubbing characteristics are hardly close to that of the practical aero-engine.

In this paper, the rotor experiment rig of aero-engine, which is designed by the Shenyang Aero-engine Design Institute, is used in the rubbing experiments. The structure design of this experiment rig is greatly improved. Firstly, its shape is consistent with core-engine's casing, and its size is treble reduced. Secondly, the internal structure is simplified, that is the core-engine is simplified to 0-2-0 support structure form and adjustable stiffness support structure is designed to adjust system's dynamic characteristics. Thirdly, multistage compressor is simplified to single-stage disk structure. Finally the experimental rig of aero-engine

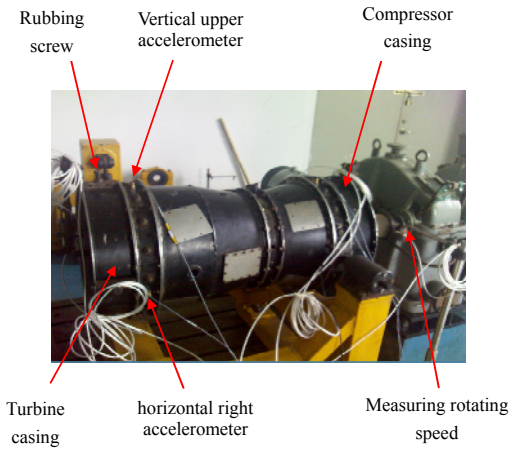

Fig. 1. The rubbing experiment of the rotor experiment rig of aero-engine.

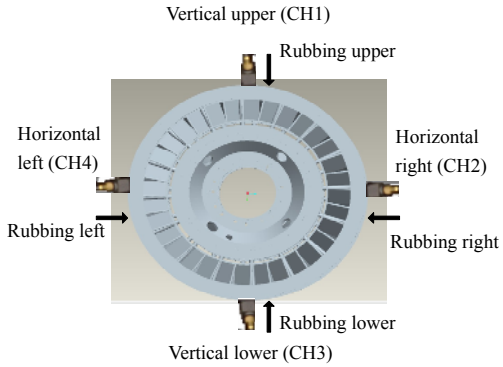

Fig. 2. The acceleration testing positions and the rubbing positions.

forms the rotor-support-blade disk -casing system in structure. The experiment rig is shown in Fig. 1.

Four rubbing screws are designed on turbine casing to carry out the rubbing experiments at the four positions. Four accelerometers are placed on the turbine casing to collect the casing acceleration signals. The rubbing positions and the installation positions of accelerometers are shown in Figs. 1 and 2. Facing to the turbine casing, the directions of rubbing positions and installation positions of accelerometers are shown in Fig. 2, which also shows the testing channels of the four accelerometers.

Six independent experiments were carried out in two days, which include three experiments on 2012-5-12, and three experiments on 2012-5-1. Four different rubbing positions were seeded, which include the upper, the lower, the left and the right. The 100 fault samples including four different rubbing positions were obtained in each experiment, and each sample includes 8192 collecting points. The sampling frequency is 10 kHz. All the experiments are carried out at 1500 rpm.

In the experiments, the rotating speed is measured by the SE series electric eddy current displacement sensors of the Southeast University Instrument Factory; the acceleration is measured by 4508 type accelerometers of the Denmark Brüel & Kjær company. The data collector is USB9234 of National Instruments Company.

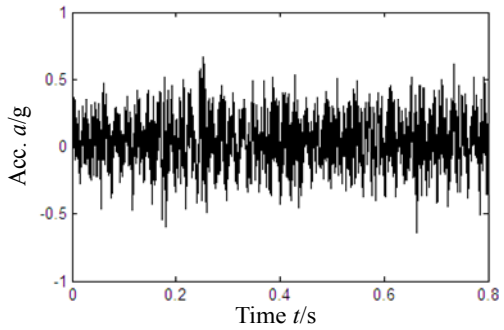

(a) Time domain waveform

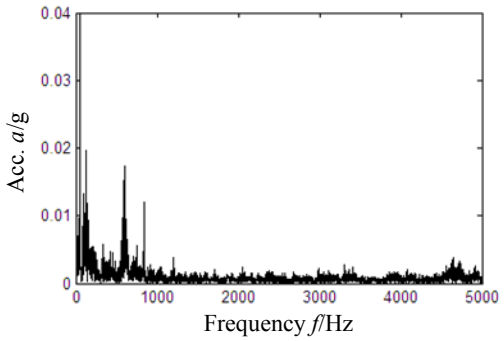

(b) Frequency spectrum

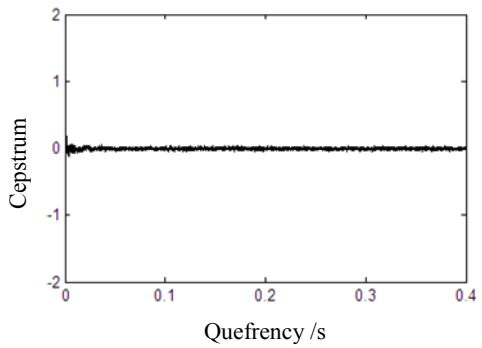

(c) Cepstrum

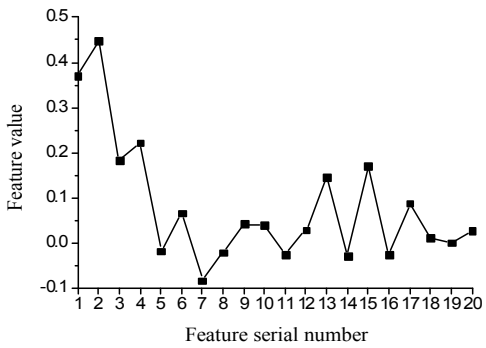

(d) Feature values (no rubbing)

Fig. 3. No rubbing.

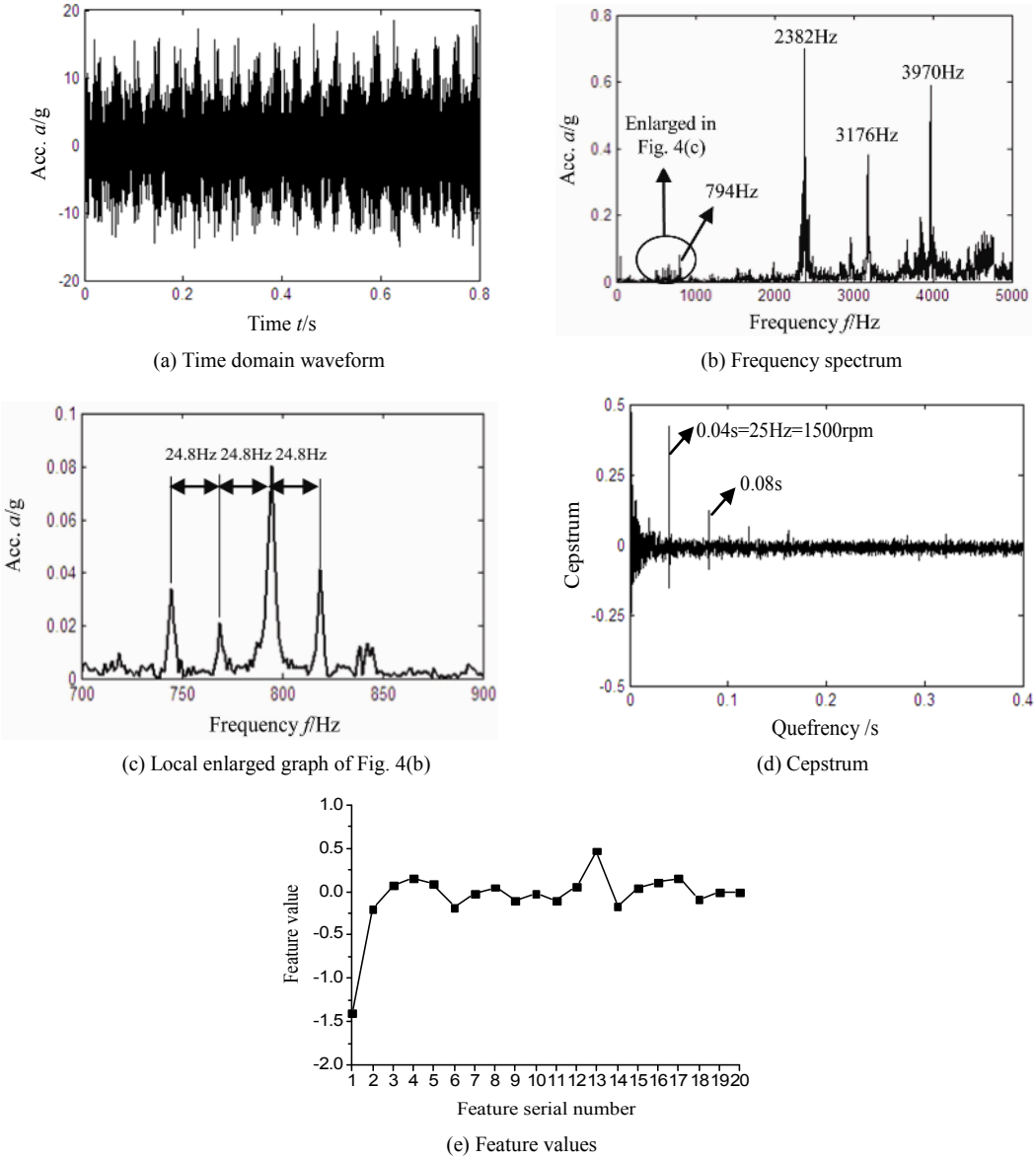

(a) Time domain waveform

(b) Frequency spectrum

(c) Local enlarged graph of Fig. 4(b)

(d) Cepstrum

(e) Feature values

Fig. 4. Rubbing upper.

4. Characteristics analysis based on casing acceleration signals

4.1 Cepstrum analysis of casing acceleration signals

The testing data of the channel 1 (CH1) on May 12th 2012 is chosen, the time domain waveform, the frequency spectrum, the cepstrum, and the 20 features extracted from the cepstrum of the acceleration signal of CH1are ploted. On condition of no rubbing, these figures are respectively shown in Figs. 3(a)-(d). By contrast, on condition that the rotor-stator rubbing position is vertical upper, these figures are shown in Figs. 4(a)-(e).

From Fig. 4, we can draw conclusions as follows:

(1) Because of the rotor disc-blade structure of the experiment rig, when the rubbing appears, every blade contacts the rubbing point in turn, and this effect will repeat once when the rotor rotates a period. Therefore, vibration caused by rubbing is similar to meshing vibration of gears, and the rubbing frequency is equal to the frequency that is the number of blades multiplies the rotating frequency. The amplitude of vibration is modulated by rotating frequency.

Therefore, there is obvious amplitude modulation feature in the frequency spectrum, which means there is sideband whose width is rotating frequency around the rubbing frequency and its multiple frequencies. The experiment rig's rotating speed is 1489 rpm, and its rotating frequency is 24.8 Hz, the number of blades is 32, and its rubbing frequency is 794 Hz. The rubbing frequency and its multiple frequencies are shown in Fig. 4(b), namely, 794 Hz, 2382 Hz, 3176 Hz, 3970 Hz, and there is many sidebands whose width is rotating frequency 24.8 Hz

around them. Fig. 4(c) is local enlarging graph of Fig. 4(b) around 794 Hz, and the sideband interval of 24.8 Hz can be obviously found around 794 Hz in Fig. 4(c).

(2) The sideband components can be summarized by cepstrum and the periodic components of frequency spectrum can be obviously shown in cepstrum. So it can simplify a group of sideband frequency band in original power spectrum into some single spectral lines, which are shown in Fig. 4(d), and the quefrency of the first single spectral line is 0.0403 s = 1/(24.8 Hz). Apparently, vibration signals modulation caused by rubbing fault can be seen in cepstrum.

(3) Comparing with casing vibration acceleration signals in the case of no rubbing, as shown in Fig. 3, it can be found that, if no rubbing appears, there is no modulation in signals, there is no quefrency component of 0.0403 s and its multiple quefrencies in cepstrum, and there is no sideband component in spectrum.

(4) From Eq. (4), it can be seen that the cepstrum reflects the combination of the transfer path and the excitation, the low quefrency components in cepstrum are the reflections of the high frequency components and high quefrency components, in contrast, are caused by the low frequency components. Because the excitation's frequency range usually is limit, in the cepstrum the less excitation components and the more transfer path components are included in the lower quefrency domain. In addition, the zero quefrency components can not reflect the system's transfer characteristics. In view of this, the real parts of the corresponding cepstrum of the first 20 quefrency points after the zero quefrency point are extracted as the features reflecting the system's transfer path characteristics. As shown in Fig. 4(e), compared with the features of no rubbing, as shown in Fig. 3(d), there is great difference between rubbing and no rubbing. The features' difference degree to rubbing positions is analyzed in detail as follows.

4.2 Feature analysis of rubbing positions identification

4.2.1 Feature analysis based on testing signals of channel 1 (CH1)

The three different experiments on May 12th 2012 are acted as examples to carry out the feature analysis. Figs. 5-8 respectively denote the features extracted from signals of CH1, and the rubbing positions are respectively the upper, the right, the lower, and the left.

From Figs. 5-8, it can be found that there is great consistency of features to the same rubbing position. The Fig. 9 denotes the feature values extracted from CH1's testing signals of different rubbing positions experiments on May 12th 2012. It can be obviously found from Fig. 9 that there is great difference among the different rubbing positions. It is because different rubbing positions reflect different transfer path. So the features for rubbing positions identification proposed in this paper have very high recognition rate to rubbing positions.

In order to further verify the effectiveness of the features, the cepstrum values from the 21st point to the 40th point and

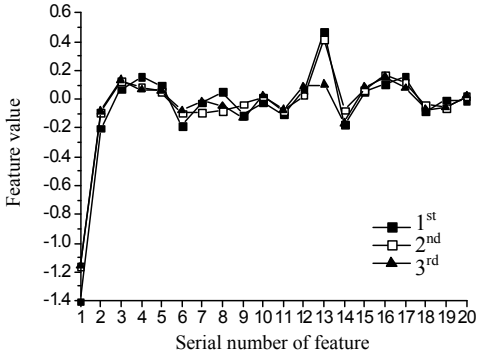

Fig. 5. Feature value (rubbing upper, CH1).

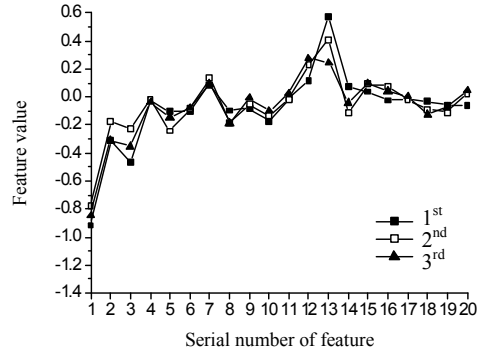

Fig. 6. Feature value (rubbing right, CH1).

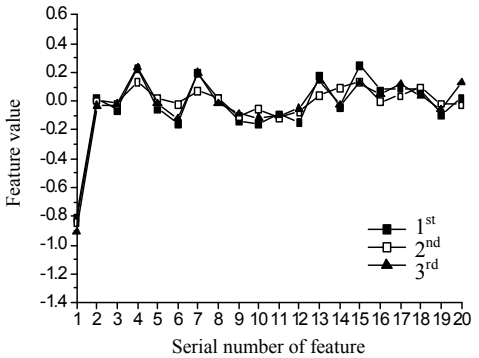

Fig. 7. Feature value (rubbing lower, CH1).

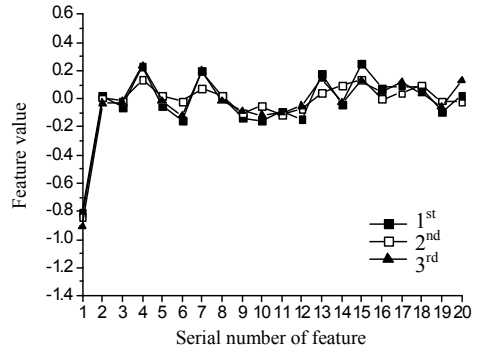

Fig. 8. Feature value (rubbing left, CH1).

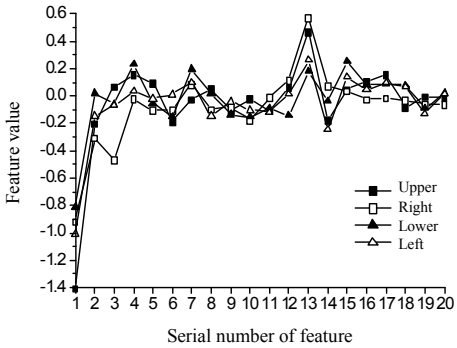

Fig. 9. Feature values of different rubbing positions (CH1).

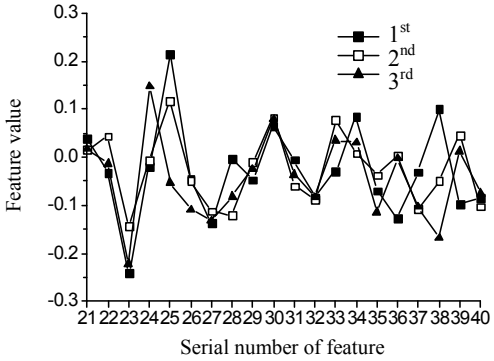

Fig. 10. Feature value (rubbing upper, CH1).

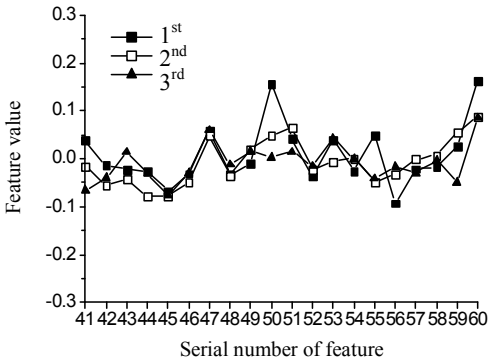

Fig. 11. Feature value (rubbing upper, CH1).

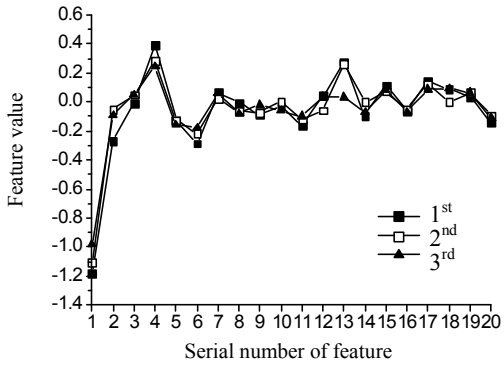

Fig. 12. Feature values (rubbing upper, CH2).

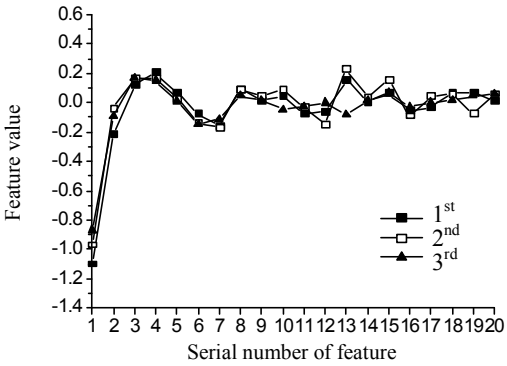

Fig. 13. Feature values (rubbing upper, CH3).

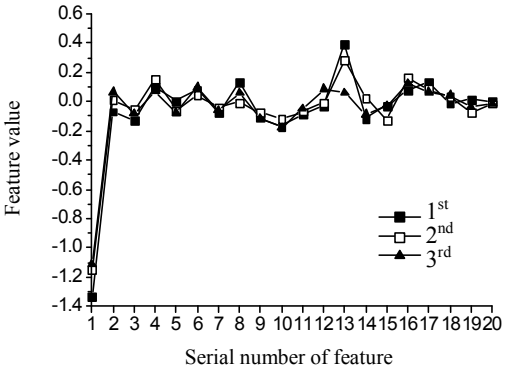

Fig. 14. Feature values (rubbing upper, CH4).

from the 41st point to the 60th points in the cepstrum are selected as the features. Figs. 10 and 11 denotes the feature values extracted from signal of CH1 when the rubbing position is upper, the experimental data comes from the three experiments on May 12th 2012. It can be found in Figs. 10 and 11 that the consistency of features becomes bad. The reason is because the effect of response in the high quefrency domain is great, while, the effect of transfer path in high quefrency domain is little. Therefore, it is the most effective to select the 1st point to the 20th point in cepstrum after the zero cepstrum point as feature values.

4.2.2 Feature analysis based on the other channels' test signals

In order to verify the effectiveness of the method further, the test data of the other channels are used to be analyzed. Firstly, experimental data with the same rubbing position (upper) coming from three different experiments on May 12th 2012 is selected. The feature values are analyzed, and shown in the Figs. 12-14. Then, in the case of different rubbing positions, the features are extracted from signals of CH2, CH3, and CH4, as shown in the Figs. 15-17.

From Figs. 12-17, just as the analysis results of CH1 signal, it can be found that the features have great consistency to the

Table 1. results of rubbing identification.

	The number of the standard sample	The number of the samples to be recognized	Recognition rate
Rubbing upper samples	100	500	100%
Rubbing right samples	100	500	100%
Rubbing lower samples	100	500	100%
Rubbing left samples	100	500	100%

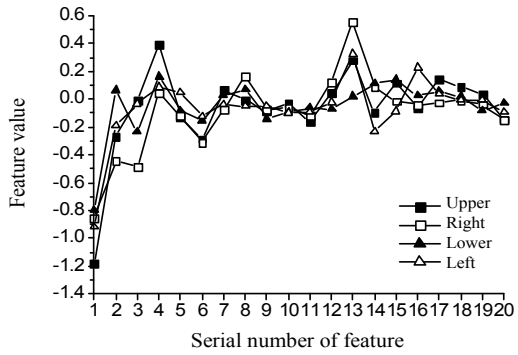

Fig. 15. Feature values (CH2).

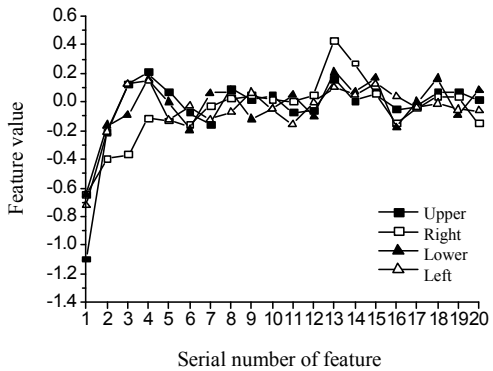

Fig. 16. Feature values (CH3).

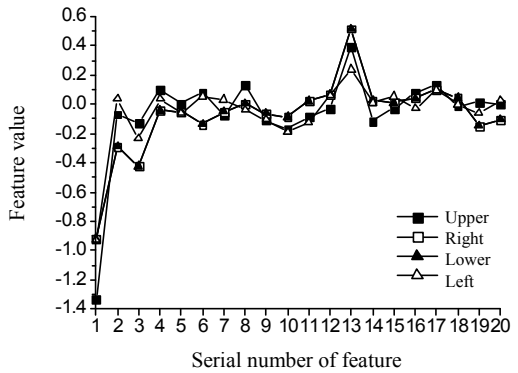

Fig. 17. Feature values (CH4).

same rubbing position and great difference to the different rubbing positions. The conclusion provides the reliable basis for effectively identifying the rubbing positions.

5. Rubbing positions identification

According to the above analysis, it can be found that method proposed in this paper has very high recognition rate to rubbing positions, and effective rubbing identification can be done through every channel. Therefore, in this paper, experimental data of channel 1 (CH1) is used in the rubbing positions identification analysis. The recognition rate is computed using the nearest neighbor classification method, and the basic steps are as follows:

(1) Features are extracted from the first experiment data on May 12th 2012, and the standard samples are formed, which includes 4 rubbing positions of the upper, the right, the lower, and the left.

(2) Features are extracted from the second and the third experimental data on May 12th 2012, and three times experimental data on May 17th 2012, and the samples to be recognized are formed, which includes 4 rubbing positions of the upper, the right, the lower, and the left.

(3) The Euclidean distance between the standard samples and the samples to be recognized is respectively calculated, and the samples to be recognized are judged as the classes of the standard sample which have closest distance with them. Finally, the recognition rate is calculated.

The results of rubbing positions identification are shown in Table 1. It can be found that features proposed in this paper has 100% recognition rate to rubbing positions, and the main reason is the features indicate the consistency to the same rubbing position and the difference to the different rubbing positions.

6. Conclusions

(1) The transfer path characteristics are separated from the vibration acceleration signals of casing by means of cepstrum analysis, and in view of this, twenty rubbing positions identification features are extracted.

(2) A large number of rubbing experiments with different rubbing positions are simulated with the rotor experiment rig of aero-engine, and the feature analysis of experimental data is carried out, and the results indicate the consistency of features to the same rubbing position and the difference of the features to the different rubbing positions.

(3) Aero-engine rubbing positions identification is carried out using the nearest neighbor classification method. The recognition rate reaches 100%, and the effectiveness of the method is fully verified.

Acknowledgment

I appreciate my graduate students Ming-yue Yu, Xiao-yong Cheng, Jing Wang, Xu-peng Li for their helps in rubbing experiments, and my graduate student Jin Wang for her some

translation work for this paper. The work is supported by the National Defence Research Program of China (No.613139) and National Natural Science Foundation of China (No. 61179057).

References

[1] A. Muszynska, Rotor-to-stationary element rub-related vibration phenomena in rotating machinery, *Shock and Vibration Digest*, 21 (1989) 3-11.

[2] Y. L. Sun, Y. X. Zhang and H. B. Chang, Method of rotor rub-impact faults diagnosis based on stator vibration signal, *Journal of Vibration Engineering*, 22 (4) (2009) 391-394 (in Chinese).

[3] F. L. Chu, Q. Y. Wang and W. X. Lu, Detective of the rub location in a rotor system with AE sensors and wavelet analysis, *Chinese Journal of Mechanical Engineering*, 38 (3) (2002) 139-143 (in Chinese).

[4] A. D. Deng, Y. Q. Bao and L. Zhao, Positioning of acoustic emission source by using sub-gradient projection based on energy attenuation model, *Chinese Journal of Mechanical Engineering*, 46 (9) (2010) 66-72 (in Chinese).

[5] F. Chu and W. Lu, Determination of the rubbing location in a multi-disk rotor system by means of dynamic stiffness identification, *Journal of Sound and Vibration*, 248 (2) (2001) 235-246.

[6] W. X. Lu, F. L. Chu and D. Guo, Rubbing location identification based on genetic algorithms, *Journal of Tsinghua University (Sci &Tech)*, 45 (2) 208-211 (in Chinese).

[7] T. He et al., Method for locating rub fault of rotor-stator based on acoustic emission beam forming, *Journal of Aerospace Power*, 26 (10) (2011) 2207-2213 (in Chinese).

[8] Q. Wang and F. Chu, Experimental determination of the rubbing location by means of acoustic emission and wavelet transform, *Journal of Sound and Vibration*, 248 (1) (2001) 91-103.

[9] S. F. Yuan and F. L. Chu, The application to shaft rubbing positions identification based on sphere support vector machine, *Journal of Vibration and Shock*, 28 (8) (2009) 70-73 (in Chinese).

[10] Q. K. Han et al., Hybrid model based identification of local rubbing fault in rotor systems, *Key Engineering Materials*, 293 (2005) 355-364.

Guo Chen received the Ph.D. from Southwest Jiaotong University, China, in 2000. He is currently a professor with the College of Civil Aviation, Nanjing University of Aeronautics and Astronautics, China. His research interests are mainly in whole aero-engine vibration, rotor dynamics, machine fault diagnosis.